J. Mt. Sci. (2014) 11(4): 967-978 e-mail: jms@imde.ac.cn http://jms.imde.ac.cn
DOI: 10.1007/s11629-012-2615-z

# Simulating Alpine Vegetation Net Primary Productivity by Remote Sensing in Qinghai Province, China

**WEI Ya-xing[1,2*], WANG Li-wen[3]**

*1 Center for Marine Economic and Sustainable Development, Liaoning Normal University, Dalian 116029, China*

*2 Liaoning Key Laboratory of Physical Geography and Geomatics, Liaoning Normal University, Dalian 116029, China*

*3 College of Urban and Environmental Science, Liaoning Normal University, Dalian 116029, China*

**Corresponding author, e-mail: wyx9585@sina.com*

**Citation:** Wei YX, Wang LW (2014) Simulating of alpine vegetation net primary productivity by remote sensing in Qinghai Province, China. Journal of Mountain Science 11(4). DOI: 10.1007/s11629-012-2615-z



**Abstract:** Primary productivity of ecosystem is important indicator about ecological assessment. Remote sensing technology has been used to monitor net primary productivity (NPP) of ecological system for several years. In this paper, the remotely sensed NPP simulation model of alpine vegetation in Qinghai Province of Tibet Plateau was set up based on the theory of light use efficiency. Firstly a new approach based on mixed pixels and Support Vector Machine (SVM) algorithm were used to correct simulated NPP values derived from Moderate Resolution Imaging Spectroradiometer (MODIS) data. Finally, spatial distribution and monthly variation characteristics of NPP in Qinghai Province in 2006 were analyzed in detail. The result showed that NPP of vegetation in Qinghai Province in 2006 ranged from 0 to 422 $gC/m^2/a$ and the average NPP was 151 $gC/m^2/a$. NPP gradually increased from northwest to southeast. NPP of different vegetation types were obviously different. The average NPP of broad-leaved forest was the largest (314 $gC/m^2/a$), and sparse shrub was the smallest (101 $gC/m^2/a$). NPP in Qinghai Province significantly changed with seasonal variation. The accumulation of NPP was primarily in the period (from April to September) with better moist and heat conditions. In July, the average NPP of vegetation reached the maximum value (43 $gC/m^2$). In our model, the advantage of traditional LUE models was adopted, and our study fully considered typical characteristics of alpine vegetation light use efficiency and environmental factors in the study area. Alpine vegetation is the most important ecological resource of Tibet Plateau, exactly monitoring its NPP value by remote sensing is an effective protection measure.

**Keywords:** Net primary productivity; Remote sensing; Light use efficiency model; Contextural approach; Support Vector Machine

**Received:** 27 November 2012
**Accepted:** 19 February 2013

## Introduction

The research on vegetation ecological characteristics is an important application field of remote sensing. Spectral characteristics of vegetation can be used to efficiently identify vegetation types from other terrestrial objects in remote sensing images. In addition, different vegetation has its own spectral characteristic which is the basis of differentiating vegetation types and estimating net primary productivity (NPP). Vegetation absorption rate is obviously different on visible and near-infrared bands, and Normalized Difference Vegetation Index (NDVI) was mentioned to express the distinction. Since Tucker et al. (1985) addressed to research relationship between NDVI with vegetation photosynthesis, remote sensing has been a main technology of observing vegetation distribution and productivity variation. Therefore, estimating vegetation NPP by remote sensing data has been an important and widely accepted research approach (Gehrung et al. 2009; Yan et al. 2004).

Estimating terrestrial vegetation NPP by remote sensing data is most prominent character of NPP model research and simulating method in the recent decade. Douglas et al. (2004) used light use efficiency (LUE) model based on remote sensing data to estimate NPP of northern temperate forest in Wisconsin, USA in 1999 and 2000. Pontus et al. (2007) constructed LUE model based on MODIS vegetation index products to calculate FPAR and NPP on Scandinavia peninsula, then they performed many experiments in the field to validate simulated results derived from the model. The U.S. National Aeronautics and Space Administration (NASA) Earth Observing System (EOS) produced the algorithm of gross primary productivity (GPP) and NPP products retrieved from MODIS data. The algorithm was in essence a modified model of LUE, since GPP was calculated from incident solar irradiance and absorptive coefficient of vegetation canopy according to the conception of LUE. The algorithm made leaf area index (LAI) retrieved from remote sensing data as a key parameter, and the consumption of autotrophic respiration was estimated through simply simulating physiological and ecological processes. Finally, GPP minus autotrophic respiration was calculated to retrieve NPP (David et al. 2006). Li et al. (2008) adopted satellite data and meteorology observing material to calculate NPP of grassland in Mongolia from 1982 to 2003 by LUE model. Guo et al. (2009) analyzed temporal and spatial variations of farmland NPP in Sanjiang Plain based on MOD17A3 dataset from 2002 to 2005. Michael et al. (2009) researched the global loss of NPP resulting from human-induced soil degradation in arid lands. Huemmrich et al. (2010) simulated tundra gross ecosystem productivity in northern Alaska, USA based on remote sensing data and LUE model, and they studied its response to various temperature and moisture conditions. Xiao et al. (2010) used GPP retrieved from MODIS to revise GPP derived from AmeriFlux data by regression trees. Comparing with other NPP estimation methods, the main advantages of NPP model based on remote sensing are: 1) rapidly update capability of multi-temporal data; 2) generalization ability of multi-scale data; and 3) extraction capacity of beyond the individual plant and non-uniform ground objects at pixel scale. Although advantages of remotely sensed NPP model are obvious, some questions should be further researched.

In this paper, typical characteristics of vegetation LUE and environment in the study area were fully taken into account, and remotely sensed NPP model of alpine vegetation based on LUE was established. Then the contextural approach based on mixed pixels and Support Vector Machine (SVM) was adopted to correct simulated NPP values. Finally, spatial distributions and temporal variations of monthly NPP in Qinghai Province in 2006 were simulated and analyzed.

## 1 The Study Area

The study area covers the whole Qinghai Province (89°35'E-103°04'E and 31°39'N-39°19'N). Qinghai Province is located in the northeastern of Qinghai-Tibet Plateau in West China (Figure 1). The climatic character in Qinghai Province is rapidly warming up in spring and fast cooling down in autumn. The average temperature in January is -13°C, and in July is 12°C. In general, precipitation is too few and very unevenly

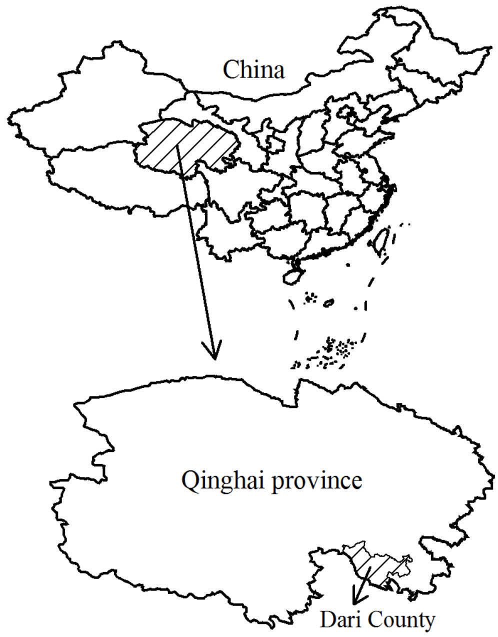


**Figure 1** Location map of the study area in China.

distributed. The trend of precipitation in Qinghai Province is gradually decreasing from southeast to northwest. The annual precipitation is about 400 mm in the southeast and only about 50 mm in Chaidamu Basin in the west. Qinghai Province is one part of Qinghai-Tibet Plateau, hence the climate has typical characteristics of Qinghai-Tibet Plateau climate. Unique natural environment in Qinghai Province determines the corresponding features of vegetation. Forest in Qinghai Province is sparse, mainly dominated by cold temperate coniferous forest and followed by temperate coniferous forest and deciduous broad-leaved forest. The area of natural grassland in Qinghai Province accounts for 50.46% of its total land area. The most widespread grassland is represented by alpine meadow. The shrubland is mainly dominated by alpine evergreen shrub and deciduous broad-leaved shrub (Shen et al. 1991).

## 2 Data Sources and Preprocessing

### 2.1 Remote sensing data

Surface Reflectance 8-Day L3 Global 500 m (MOD09A1), Land Surface Temperature/ Emissivity 8-Day L3 Global 1km (MOD11A2), Land Cover Type Yearly L3 Global 1km (MOD12Q1), Vegetation Indices 16-Day L3 Global 1 km (MOD13A2), Leaf Area Index/FPAR 8-Day L4 Global 1km (MOD15A2), Gross Primary Productivity 8-Day L4 Global 1km (MOD17A2), and Albedo 16-Day L3 Global 1km (MOD43B3) of MODIS land products were used in the paper to calculation and validation during the construction of NPP model. They were provided by LPDAAC (Land Process Distributed Active Archive Center, U.S.A). Preprocessing procedure includes: MRT software programmed by USGS EROS data center was adopted to accomplish images mosaicking, geometric rectification and resampling; above multi-temporal MODIS data products were synthetically pretreated by Maximum Value Composite (MVC), that is, the value of each pixel in images was respectively replaced with the maximum value of this pixel for j days in order to reduce the effect from atmospheric clouds, particles, shadows, perspective and solar altitude angle; pixels with abnormal values in MODIS products were repaired by the linear relationship of adjacent temporal image.

TM data used in the study were received by Landsat-5 launched on March 1, 1984. 5 scenes of TM images covering the whole Dari County were selected, of which path/row numbers were 132/37, 133/36, 133/37, 134/36 and 134/37, respectively. Since receiving time of chosen TM images were all in July, images were better representative of reflecting the good period of vegetation growth in a year. And selective images with good quality ensured operability of image analysis and reliability of results. Geometric and atmosphere corrections were made to selected TM images. FlAASH (Fast Line-of-sight Atmospheric Analysis of Spectral Hypercube) was used as atmospheric correction method. After TM images were processed by FLAASH, their contrast was enhanced due to removing some mist. Images did not show obvious change on visual effects after atmospheric correction, but their spectral characteristics were very different.

### 2.2 Meteorology data

Various meteorological parameters were needed to input the NPP model. Meteorology data from 41 stations in Qinghai Province, such as average temperature (0.1°C), precipitation (0.1 mm), average atmospheric relative humidity (%), sunshine duration (0.1 h), air pressure (0.1 hpa) and mean wind speed (0.1 m/s), were provided by Chinese Meteorological Center. Processing steps of meteorological grid maps were as follows: 1) according to latitude and longitude information provided by data, various meteorological data were converted to spatial vector data with geographical coordinates; 2) required parameters were added into vector data as attribute fields; and 3) Kriging interpolation algorithm were performed to meteorological vector data.

### 2.3 Land cover classification map

The land cover classification map of Qinghai Province has been published by Journal of Geographical Sciences (Wang et al. 2008), and it was adopted in this study. Based on field investigation and various methods of land cover classification, the classification approach of

Qinghai Province synthesized supervised classification, unsupervised classification and decision tree classification. There are 14 land cover classes in Qinghai Province, such as city, water body, snow/ice, desert, Gobi, dense grassland (DG), needle-leaved forest (NLF), broad-leaved forest (BLF), sparse grassland (SG), dense shrub (DS), sparse shrub (SS), middle density grassland (MDG), grassland mixed with farmland (GMF), and needle-leaved and broad-leaved mixed forest (NLBLMF). Vegetation distributions, especially sparse vegetation distributions (including sparse grassland and sparse shrub), were emphasized in this classification approach.

### 2.4 Measured data

Measured data were used in the study, and they were gotten from the experiment conducted in Dari County of Qinghai Province. Grasslands were main experimental objects. Field investigations were taken in July 2006, because July was the best period of vegetation growth status. In the process of field investigations, Global Position System (GPS) was used to precisely locate typical sites. Then vegetation in the site was compared with remote sensing image, and vegetation types and cover status were recorded. The experiment mainly included: LI-6400 portable photosynthesis system was used to measure some physiological indicators of typical grasslands on Qinghai-Tibet Plateau, such as net photosynthetic rate, stomata conductance, transpiration rate, leaf temperature, and so on; SUNSCAN canopy analysis system was applied to observe incident photosynthetic active radiation (PAR) (including direct PAR and scattering PAR), PAR at the bottom of the canopy, etc; LAI-2000 vegetation canopy analysis system was used to measure LAI of typical grasslands; and grassland plots were reasonably chosen to measure the biomass.

## 3 Methods

### 3.1 The construction of NPP model

Remotely sensed NPP model based on LUE has significant advantages of obtaining model parameters through remote sensing and be suitable to regional and global scale. Therefore, remotely sensed NPP model constructed in the study was based on LUE theory. It draws on advantages of many LUE models (e.g. MODIS-PSN, CASA, GLO-PEM and VPM), while it fully considers typical characteristics of vegetation LUE and environmental factors for specific region.

Remotely sensed *NPP* model can be expressed as:

$$NPP = PAR \times FPAR \times \min(T_s,\ W_s) \times \varepsilon_{\max} \quad (1)$$

where *PAR* is photosynthetic active radiation (MJ/m²), *FPAR* is fractional photosynthetic active radiation (unitless), $T_s$ is temperature stress factor (unitless), $W_s$ is water stress factor (unitless), and $\varepsilon_{\max}$ is maximum LUE (gC/MJ).

Figure 2 shows the flowchart of calculating NPP.

#### 3.1.1 Maximum LUE ($\varepsilon_{\max}$)

According to literature and field experimental data, the study first collected a set of observational data including NPP, PAR, FPAR, temperature stress factor, and water stress factor for some vegetation. Afterwards, maximum likelihood estimate was adopted to simulate the value of maximum LUE for the vegetation (Zhu et al. 2006; Li et al. 2004; Pu et al. 2005).

Maximum likelihood estimate is used to assume that *V* is the residual of *NPP* and $\hat{\varepsilon}_{\max}$ is simulated value of maximum LUE ($\varepsilon_{\max}$). So the error equation is:

$$V = PAR \times FPAR \times \min(T_s,\ W_s) \times \hat{\varepsilon}_{\max} - NPP \quad (2)$$

The simulated value ($\hat{\varepsilon}_{\max}$) of maximum LUE ($\varepsilon_{\max}$) is finally deduced as:

$$\hat{\varepsilon}_{\max} = \frac{\sum_{i=1}^{n} x_i y_i - n\overline{xy}}{\sum_{i=1}^{n} x_i^{2} - n\overline{x}^{2}} \quad (3)$$

where $\hat{\varepsilon}_{\max}$ is the simulated value of maximum LUE, $x_i$ is the calculated value of $PAR \times FPAR \times \min(T_s,\ W_s)$ for the plant, $y_i$ is the NPP value for the plant, *i* is the sample number for the plant, *n* is maximum sample number for the

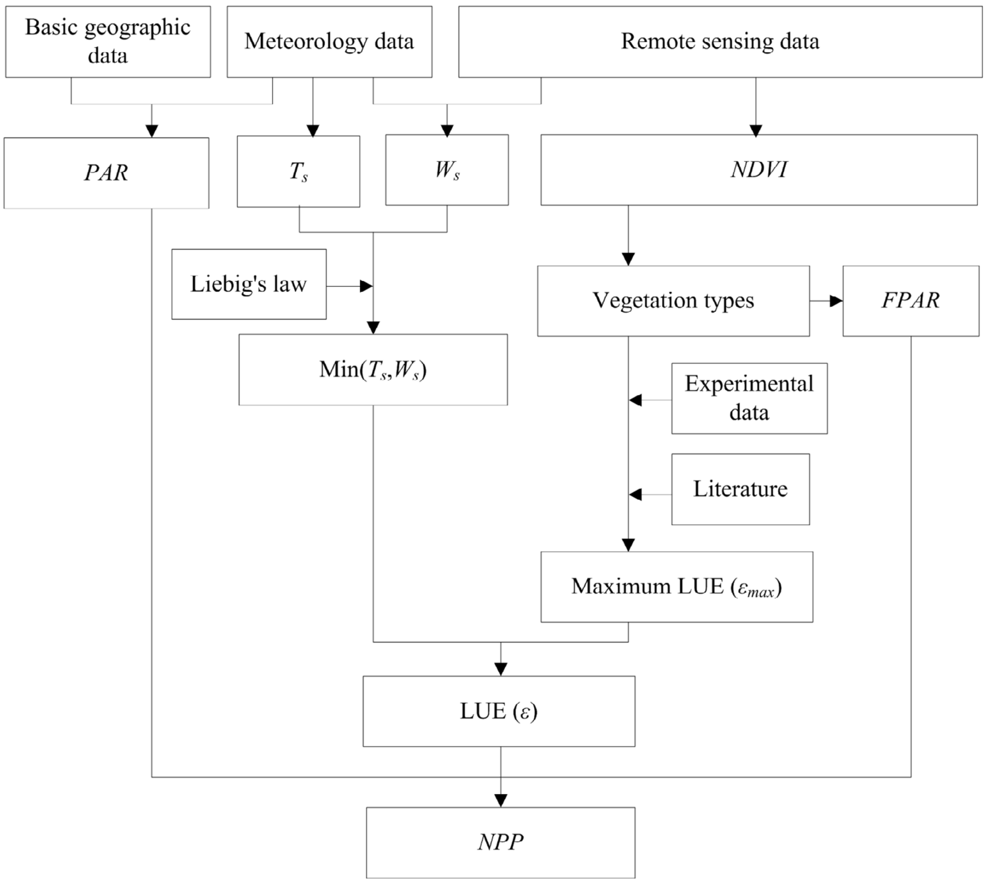


**Figure 2** Flowchart of net primary productivity (NPP).

plant, $\bar{x} = \frac{1}{n}\sum_{i=1}^{n} x_i$ , and $\bar{y} = \frac{1}{n}\sum_{i=1}^{n} y_i$ .

In order to improve the simulation precision of maximum LUE ($\varepsilon_{max}$) for various remotely sensed grassland and shrubland classes, the weight average value of maximum LUE values for main grass or shrub classes is calculated as the maximum LUE value of corresponding remotely sensed grassland or shrubland class:

$$\varepsilon_{\max} = \sum_{i=1}^{n} c_i \left(\hat{\varepsilon}_{\max}\right)_i \quad (4)$$

where $c_i$ is area fraction of $i$ grass (or shrub), $\left(\hat{\varepsilon}_{\max}\right)_i$ is simulated maximum LUE value of $i$ grass (or shrub), $i$ refers to $i$ grass (or shrub), and $n$ is the number of main grass (or shrub) classes.

### 3.1.2 FPAR

The nonlinearity relationship between FPAR and spectral vegetation index has been proven by many researches. Simple ratio (SR) and NDVI are two most common indices. The nonlinearity relationship between FPAR and NDVI illustrates the widely proposed phenomenon that NDVI is saturated when LAI is greater than 3. And it also implies the linear relationship between FPAR and SR (Chen et al. 2007). The relationship equation between FPAR and SR was constructed based on data in the study area:

$$FPAR = \min\left[\frac{SR}{SR_{\max} - SR_{\min}} - \frac{SR_{\min}}{SR_{\max} - SR_{\min}}, 0.95\right] \quad (5)$$

where $SR_{min}$ is assigned to a same value of 1.06 for all vegetation types, the value of $SR_{max}$ is related to the vegetation type: 6.14 for broad-leaved forest, 3.88 for needle-leaved and broad-leaved mixed forest, 3.44 for needle-leaved forest, 3 for dense grassland, 3.27 for dense shrub, 2.17 for middle density grassland, 1.94 for grassland mixed with farmland, 1.78 for sparse grassland, and 1.70 for sparse shrub.

### 3.1.3 Water stress factor ($W_s$)

Water effect on photosynthesis is usually expressed by the formula of vapor pressure deficit (VPD) and soil moisture in some productivity models. But these two parameters are difficult to be accurately determined. In this study, evaporative fraction (EF) was used to estimate water stress factor. EF can better characterize water condition of ecosystems, and it also can be easily retrieved from remotely sensed vegetation indices and land surface temperature products (Yuan et al. 2007; Venturini et al. 2004). EF can be given by:

$$W_s = EF = \frac{LE}{LE + H} \tag{6}$$

where $W_s$ is water stress factor, $LE$ is latent heat flux (W/m$^2$), and $H$ is sensible heat flux (W/m$^2$).

### 3.1.4 Temperature stress factor ($T_s$)

The method derived from the Terrestrial Ecosystem Model (TEM) was used to estimate temperature stress factor (Akihiko, 2008):

$$T_s = \frac{(T - T_{\min})(T - T_{\max})}{(T - T_{\min})(T - T_{\max}) - (T - T_{opt})^2} \tag{7}$$

where $T$ is air temperature, $T_{min}$, $T_{opt}$ and $T_{max}$ are minimum, optimum and maximum temperature of photosynthesis, respectively. If air temperature is below $T_{min}$ or above $T_{max}$, $T_s$ will be set to 0°C. In the study, $T_{min}$ and $T_{max}$ were assigned to 0°C and 36°C, respectively. In addition, assuming that plants have adapted well to growth environmental temperature, $T_{opt}$ may be set to long-term average temperature of the growing season.

## 3.2 Correction of simulated NPP

In this paper, vegetation NPP in Qinghai Province in 2006 was simulated by remote sensing model. Due to lower spatial resolution of MODIS data, simulated NPP values need to be modified. The contextural approach based on mixed pixels proposed by Anita et al. (2004) and SVM algorithm were used to correct simulated NPP values retrieved from MODIS data in the study.

The contextural approach based on mixed pixels considers spatial heterogeneity issues existing in mixed pixels. It utilizes land cover data at high resolution to calculate area fractions of dominant pixels in mixed pixels at low resolution, then it uses scale effect correction factor to correct simulated NPP values retrieved from Low-resolution remote sensing data. The study assumes that simulated NPP values from TM represent the true value of vegetation NPP and simulated $NPP_{MODIS}$ from MODIS are approximate NPP values needed to be corrected. Based on simulated NPP results retrieved from high-resolution remote sensing data of TM, $NPP_{MODIS\,j\_corrected}$ can be achieved by scale effect correction to $NPP_{MODIS}$ derived from low-resolution remote sensing data of MODIS. Thus the precision of estimating NPP from remote sensing data at low resolution can be improved. The formula of correcting simulated NPP retrieved from MODIS data is:

$$NPP_{MODIS\,j\_corrected} = NPP_{MODIS\,j} \times \left(1 - \sum_{i=1}^{n} C_{ij} F_{ij}\right) \tag{8}$$

where $F_{ij}$ is the fraction of nondominant cover type $i$ (in 30m-resolution TM images) in a pixel labeled as cover type $j$ (in 1km-resolution images converted from 30m-resolution TM images), $C_{ij}$ is the regression coefficient between $R_j$ (scale-effect correction factor) for a pixel labeled as cover type $j$ and $F_{ij}$ of nondominant cover type $i$ in this pixel, $n$ is the number of nondominant cover types in a pixel labeled as cover type $j$, and $NPP_{MODIS\,j}$ is simulated NPP results retrieved from low-resolution remote sensing data of MODIS for a pixel labeled as cover type $j$.

In the process of correcting simulated NPP values, regression coefficient $C_{ij}$ between $R_j$ (scale-effect correction factor) for a pixel labeled as cover type $j$ and $F_{ij}$ of nondominant cover type $i$ in this pixel needs to be calculated. In this paper, SVM algorithm was adopted to establish the regression model between $R_j$ and $F_{ij}$. SVM is especially suitable for limited sample. Its goal is to get the optimal solution under existing information rather than the optimal solution that the amount of information tends to infinity. The algorithm eventually transforms into a problem of quadratic optimization, and it solves the inevitable problem of local extremum in neural network. SVM algorithm transforms the actual problem into high dimensional feature space by the nonlinear transformation, and it constructs a linear function in high dimensional space to realize nonlinear discriminant function in the original space. SVM skillfully solves the dimension problem, and it makes the algorithm complexity independent of the sample dimension. Libsvm software adopted in the paper can solve problems of classification, regression, distribution estimation, etc, and it provides four common kernel functions including linear, polynomial, RBF, and S-shaped functions (Lin 2008).

## 4 Results

### 4.1 Comparison and validation of simulated vegetation NPP in Qinghai Province

Nowadays different scholars have obtained different simulated NPP values by different methods, so the validation of simulated NPP is very important. In addition, NPP affected by geographical and environmental factors fluctuate in different years, so real-time ground measured data are the best data of validating results derived from the NPP model. However, as it is impossible to measure NPP at large areas at the same time (especially at the regional or even global scale), so most validations of simulated NPP results are only accomplished through indirect approaches.

To validate the correctness of estimated NPP results in this paper, comparison and validation to simulated NPP have been performed through three aspects: 1) comparison with MODIS17A2 of NPP products in 2006; 2) comparison with relative simulated NPP results derived from other studies; and 3) comparison with field measured data.

(1) Comparison between simulated NPP results in this paper and MODIS17A2 products in 2006;

(2) Figure 3 shows vegetation NPP distributions in Qinghai Province in 2006 derived from MOD17A2. Comparing with simulated NPP in the study (Figure 4), the result shows: in MOD17A2, the average NPP of vegetation in Qinghai Province in 2006 was 90 gC/m²/a, and NPP ranged from 0 to 794 gC/m²/a. But the mean NPP simulated in the study was 151 gC/m²/a, and NPP ranged from 0 to 422 gC/m²/a. From the view of the spatial distribution of NPP, most parts of Qinghai Province are yellow (less than 100 gC/m²/a) in

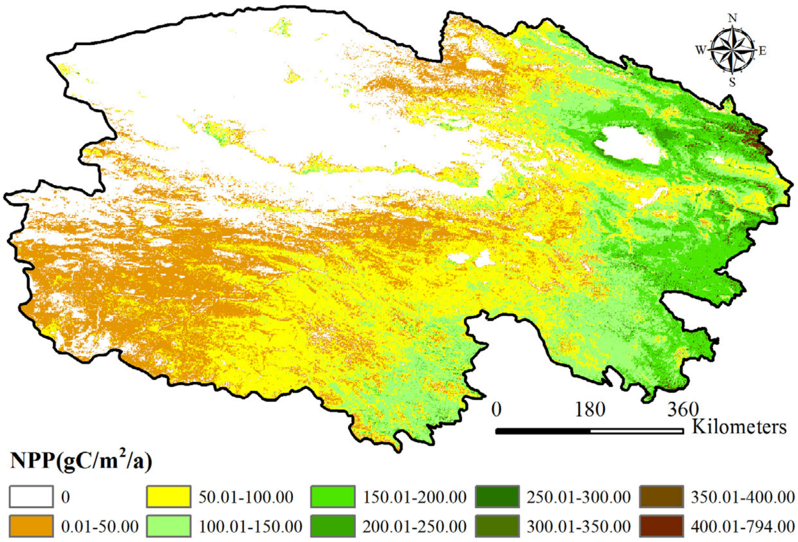


**Figure 3** The spatial distribution map of vegetation NPP in Qinghai Province in 2006 (MOD17A2).

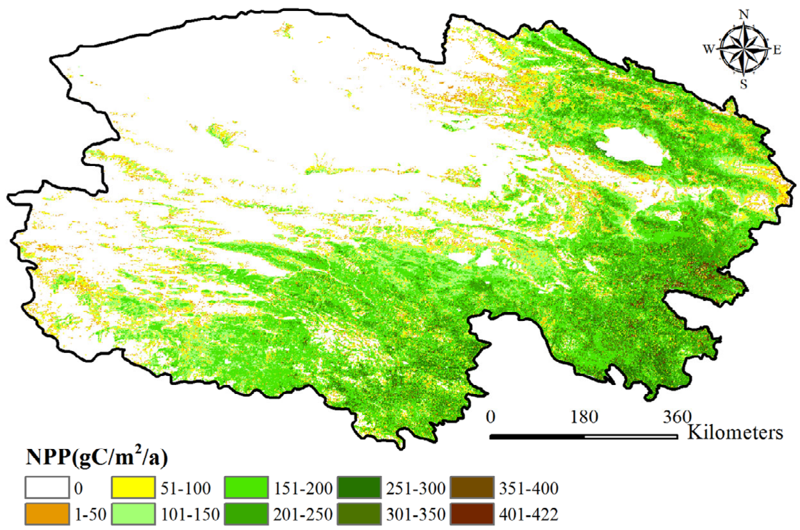


**Figure 4** The spatial distribution map of vegetation NPP in Qinghai Province in 2006 (our result).

MOD17A2, and NPP values are significantly lower than simulated NPP values in the study. In addition, in brownish red regions of eastern Qinghai Province in MOD17A2, NPP are generally greater than 400 gC/m²/a, and these areas should be forest cover regions. However, in contrast with relative vegetation distribution map, there are no large areas of forest in these regions. Only a small area of forest exists, and forests are scattered.

(3) Comparison with results derived from similar studies

Simulated NPP results of main vegetation types derived from various researchers are quite different. Years, data sources, used models, model steps, selected vegetation type maps, and the size of grid may affect simulation results. Therefore, large regional NPP estimates put forward higher requirements for data sources and the stability of estimation methods. Other researchers simulated the average NPP of various vegetation types in the China region or in the entire Qinghai-Tibet Plateau, but their study only estimated the mean NPP of different vegetation types in Qinghai Province. Due to the influence of geographical location and climatic conditions, simulated NPP values in this paper are less than national estimated NPP values, and they are closer to the estimation results of NPP in relatively small study area of Qinghai-Tibet Plateau.

(4) Comparison with the measured data

Grassland is the most important vegetation type in Qinghai Province. So this study focuses on the validation to NPP of grassland ecosystem simulated by the model. The validation of grassland NPP first used the observation data derived from the station of observing alpine meadow ecosystem flux in Haibei Prefecture of Qinghai Province (Yu et al. 2008). 3 sets of eddy covariance observing system were erected around Haibei station to observe *Kobreisa humilis, Potentilla fruticosa* and *Kobresia tibetica*. Observations show that NPP was 132 gC/m²/a for *Kobreisa humilis*, 131 gC/m²/a for *Kobresia tibetica*, and 124 gC/m²/a for *Potentilla fruticosa*, respectively. The average value of them was 129 gC/m²/a. Simulated NPP value at the corresponding coordinate in our study was 172 gC/m²/a.

As it is very difficult to measure NPP, NPP data converted from biomass are often used instead of measured NPP data. In the study, grassland biomass data measured in Dari County of Qinghai Province in July 2006 were converted to NPP values. Spatial locations of measured NPP data and simulated NPP data were matched, and accuracy test of simulated values was implemented (Figure 5). Test results showed that simulated values were consistent with measured values ($R^2$=0.9348).

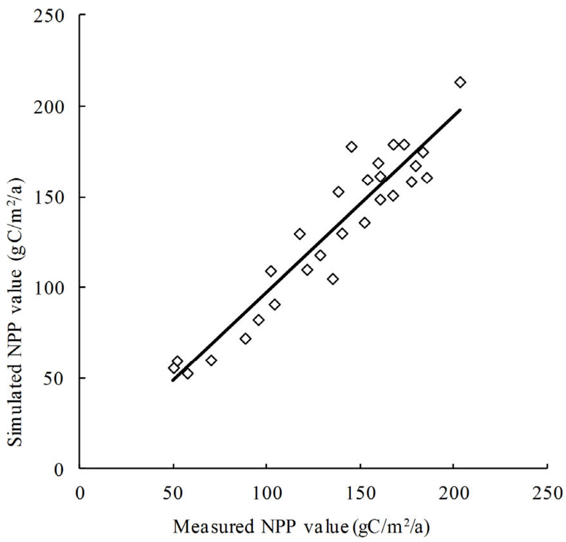


**Figure 5** Comparison of simulated NPP value and measured NPP value.

## 4.2 The spatial distribution characteristics of vegetation NPP in Qinghai Province

Qinghai Province with high altitude and cold climate is a component of Qinghai-Tibet Plateau. The specific natural environment decides that local vegetation has the characteristic of adapting to alpine environment. Meanwhile, due to the restriction of the harsh natural environment, comparing with vegetation at the same altitude in the eastern region of China, vegetation in Qinghai Province with relatively short growing season and slow bioaccumulation has comparatively low NPP.

From the spatial distribution map of vegetation NPP in Qinghai Province in 2006, it was showed that estimation results of vegetation NPP in Qinghai Province in 2006 ranged from 0 to 422 gC/m²/a and the average NPP was 151 gC/m²/a. NPP gradually increased from northwest to southeast. Vegetation NPP in most regions of northwestern Qinghai Province which was desert and Gobi (e.g. Chaidamu Basin) were low and ranged from 40 to 80 gC/m²/a (such as 71 gC/m²/a in Golmud). NPP of vegetation in the southeast were high and ranged from 174 to 401 gC/m²/a (such as 298 gC/m²/a in Dari County, 367 gC/m²/a in Maqin County, 376 gC/m²/a in Gander County). NPP in the south of Qinghai Province were also high and ranged from 152 to 350 gC/m²/a (such as 250 gC/m²/a in Yushu County, 236 gC/m²/a in Qumalai County, 325 gC/m²/a in Nangqian County). NPP of vegetation around Qinghai Lake were high and varied from to 336 gC/m²/a (such as 214 gC/m²/a in Huangyuan County, 193 gC/m²/a in Gangcha County, 203 gC/m²/a in Haiyan County). From the statistics, NPP values in the southeast, the south and regions around Qinghai Lake were larger than other areas of Qinghai Province.

Administrative divisions of Qinghai Province include Xining City, Haidong Prefecture, Haibei Tibetan Autonomous Region, Hainan Tibetan Autonomous Region, Huangnan Tibetan Autonomous Region, Guoluo Tibetan Autonomous Region, Yushu Tibetan Autonomous Region, and Haixi Mongolian Tibetan Autonomous Region. Total NPP of vegetation in Qinghai Province in 2006 were 60.33 TgC/a. NPP in various administrative division regions were largely different (Figure 6). Annual total NPP of vegetation in Yushu Tibetan Autonomous Region were the largest (20.84 TgC/a), and they accounted for about 35.2% of Qinghai Province's annual total NPP. Guoluo Tibetan Autonomous Region with annual total NPP of 14.87 TgC/a was second (25.7%). Haixi Mongolian Tibetan Autonomous Region with annual total NPP of 6.83 TgC/a was third (11.4%). Annual total NPP of vegetation in Xining City were least (1.33 TgC/a), and they accounted for about 2.3%. The average NPP per unit area in Huangnan Tibetan Autonomous Region was the largest (255 gC/m²/a). The second largest average NPP per unit area was in Guoluo Tibetan Autonomous Region (218 gC/m²/a), followed by Xining City (185 gC/m²/a). Next, in the order of the decreasing average NPP per unit area, the remaining regions were Haibei Tibetan Autonomous Region (177 gC/m²/a), Hainan Tibetan Autonomous Region (168 gC/m²/a), Yushu Tibetan Autonomous Region (162 gC/m²/a), Haidong Prefecture (131 gC/m²/a) and Haixi Mongolian Tibetan Autonomous Region (97 gC/m²/a).

NPP of various vegetation types are obvious different. The average NPP per unit area of forests was the highest. Among forests, the average NPP per unit area for broad-leaved forest was the largest (314 gC/m²/a), followed by needle-leaved and broad-leaved mixed forest (279 gC/m²/a), and then needle-leaved forest (267 gC/m²/a). Next, in the order of the decreasing average NPP per unit area, the remaining vegetation types were dense shrub (213 gC/m²/a), dense grassland (194 gC/m²/a), middle density grassland (157 gC/m²/a), grassland mixed with farmland (146 gC/m²/a), sparse grassland (121 gC/m²/a), and sparse shrub (101 gC/m²/a). Based on areas covered by different vegetation types, total NPP of various vegetation types were calculated, respectively. The total NPP of dense grassland was the largest (18.32 TgC/a) (1Tg=$10^{12}$g), followed by grassland mixed with farmland (18.00 TgC/a), and then middle density grassland (15.42 TgC/a). Next, in the order of the decreasing total NPP, the remaining vegetation types were dense shrub (3.51 TgC/a), sparse grassland (2.36 TgC/a), sparse shrub (1.57 TgC/a),

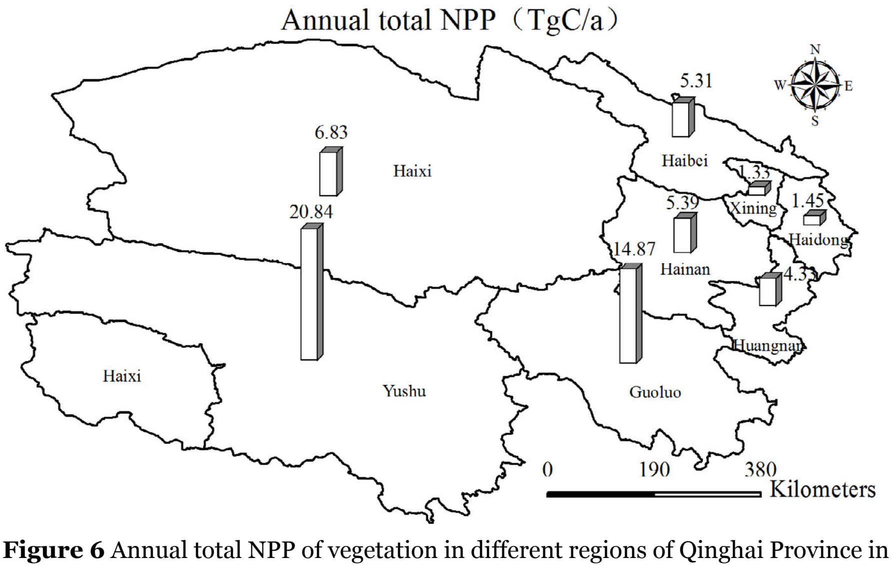


**Figure 6** Annual total NPP of vegetation in different regions of Qinghai Province in 2006.

needle-leaved forest (0.55 TgC/a), needle-leaved and broad-leaved mixed forest (0.31 TgC/a) and broad-leaved forest (0.30 TgC/a). Annual total NPP of the whole grassland ecosystem including sparse grassland, middle density grassland and dense grassland was 36.1 TgC/a, and it accounted for about 59.9% of the total NPP in Qinghai Province. Annual total NPP of shrubland ecosystem including sparse shrub and dense shrub was 5.08 TgC/a (8.4% of Qinghai Province's annual total NPP). Annual total NPP of forest ecosystem including needle-leaved forest, needle-leaved and broad-leaved mixed forest, and broad-leaved forest was 1.16 TgC/a (1.9%).

### 4.3 Monthly variable characteristics of vegetation NPP in Qinghai Province

Figure 7 shows that NPP of Qinghai Province significantly changed with seasonal variation. The maximum value of NPP was 61 gC/m² in July. Under various conditions of water and heat, NPP in each month of a year is different. From late March, temperatures began to rise above 0°C during the day, and frozen soil began to melt from the surface. So the phenomenon of melting during the day and freezing at night appeared. Due to different radiation absorptions and transmissions for various vegetation types, the driving influences from frozen soil and vegetation cover were different on soil energy distribution. Regional NPP values evidently increased, and the average NPP of vegetation reached 15 gC/m² in March. From March to April, regional frozen soil was in the process of spring melting, and vegetation also grew as temperature increased. In April, the mean NPP of vegetation increased to 26 gC/m². From May to June, water, light and heat started to became adequate. The growth of vegetation was into the development period, and the value of NPP increased rapidly. In May, vegetation NPP increased rapidly to 38 gC/m². Affected by the impact of less precipitation in June, the average NPP of vegetation slightly decreased to 35 gC/m². In July, the growth of vegetation was the most luxuriant, and vegetation NPP reached the maximum value (43 gC/m²). From August to September, vegetation was in final growth period and leaves started to turn yellow or to physiological maturity, then NPP in August was 39 gC/m². From late September, vegetation in the study area began to rapidly wither due to the sharp decline of temperature. The soil took on different degrees of

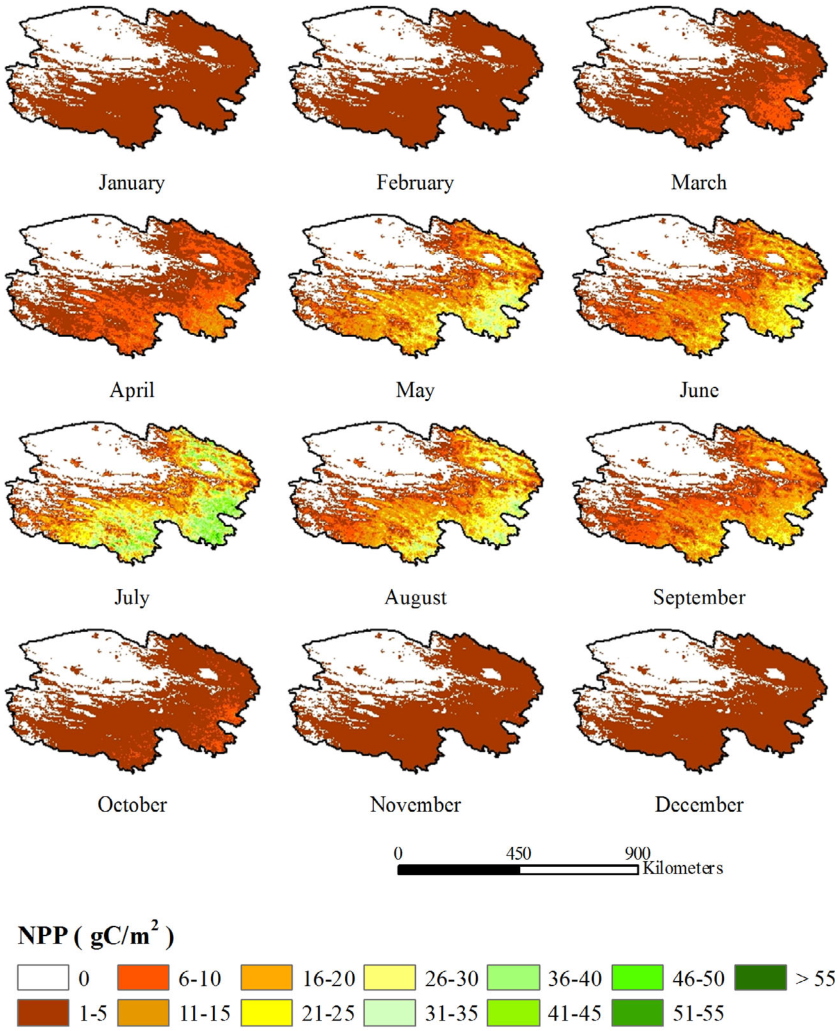


**Figure 7** The monthly variable map of vegetation NPP in Qinghai Province in 2006.

freezing, and water absorption capacity of vegetation sharply declined. In September, the average NPP of vegetation decreased rapidly to 30 gC/m$^2$. From late November, vegetation withered and water was in the solid-ice state, so NPP was very small at this stage. The average NPP of vegetation in Qinghai Province in winter was generally less than 8gC/m$^2$. It can be seen that the accumulation of NPP mainly occurred from April to September with good water and heat. The amount of NPP for these 6 months accounted for 79.8% of annual total NPP. From the perspective of seasonal changes, seasonal average NPP in Qinghai Province was 79 gC/m$^2$ in spring (29.8%), 117 gC/m$^2$ in summer (44.3%), 51 gC/m$^2$ in autumn (19.2%), and 18 gC/m$^2$ in winter (6.7%), respectively.

The results showed that NPP variations of three kinds of grasslands in 2006 present the similar trend. NPP from April to September was obviously larger than NPP in other months. NPP of sparse grassland was about 10 gC/m$^2$; NPP of middle density grassland was about 15 gC/m$^2$; and NPP of dense grassland was about 20 gC/m$^2$. The accumulation of NPP was primarily in the period (from April to September) with better water and heat conditions. The accumulation ratio of NPP (NPP accumulated for these 6 months divided by annual total NPP) was 73.9% for sparse grassland, 74.5% for middle density grassland, and 72.8% for dense grassland, respectively. NPP reached the highest value in July (e.g. 19 gC/m$^2$ for sparse grassland, 30 gC/m$^2$ for middle density grassland, 36 gC/m$^2$ for dense grassland). In the growing season, NPP had the largest increase from April to July, and NPP had the biggest decline from August to October. In June, affected by less precipitation, NPP of grasslands was slightly lower than NPP in May or July (e.g. 16 gC/m$^2$ for sparse grassland, 19 gC/m$^2$ for middle density grassland, 26 gC/m$^2$ for dense grassland).

The variable tendency of shrubland NPP was similar to that of grassland. NPP in the period (from April to September) was evidently larger than NPP in other months. NPP of sparse shrub was about 8 gC/m$^2$, and NPP of dense shrub was about 21 gC/m$^2$. The accumulation of NPP was mainly in the period (from April to September) with better water and heat environment. The accumulation ratio of NPP (NPP accumulated for these 6 months divided by annual total NPP) was 76.3% for sparse shrub and 72.3% for dense shrub, respectively. The value of NPP was the largest in July (e.g. 17 gC/m$^2$ for sparse shrub, and 42 gC/m$^2$ for dense shrub). NPP from April to July had the largest increase, and NPP from August to October had the biggest decline. Restricted by less water, NPP of shrubland in June was appreciably less than NPP in May or July (e.g. 12 gC/m$^2$ for sparse shrub, and 35 gC/m$^2$ for dense shrub). In winter, NPP of sparse shrub was about 4 gC/m$^2$, and NPP of dense shrub was about 13 gC/m$^2$.

## 5 Conclusion

(1) Estimations of various input parameters for remotely sensed NPP models consider vegetation LUE and environment in the study area in detail. Therefore, simulated NPP results in this paper are more accurate than other simulations.

(2) Simulated maximum LUE of main vegetation types by maximum likelihood estimate are based on literature and measured NPP data, so they are in accord with the real situation in the study area. In addition, as grassland is the main vegetation type in the study area, simulations of grassland maximum LUE are specially processed to reduce errors.

(3) The calculation of environmental influence factors is simpler, and spatial distribution trends reflected by them conform to actual situations.

(4) Simulated NPP derived from low-resolution remote sensing data of MODIS are corrected by SVM algorithm and the contextural approach based on mixed pixels in order to improve the effect on the NPP model from scale effect.

## Acknowledgements

This study was funded by the National Natural Science Foundation of China (Grant No. 41271421), and the Humanities and Social Sciences Research Project of the Ministry of Education in China (Grant No. 10YJCZH156).

## References

Akihiko I (2008) The regional carbon budget of East Asia simulated with a terrestrial ecosystem model and validated using AsiaFlux data. Agricultural and Forest Meteorology 148(5): 738-747. DOI: 10.1016/j.agrformet.2007.12.007

Anita S, Chen J, Liu J (2004) Spatial scaling of net primary productivity using subpixel information. Remote Sensing of Environment 93(1-2): 246-258. DOI: 10.1016/j.rse.2004.07.008

Chen L, Gao Y, Li L (2007) Net primary production estimation of forest based on MODIS data. Chinese Science D: Earth Science 37(11): 1515-1521. (In Chinese)

David PT, William DR, Warren BC (2006) Evaluation of MODIS NPP and GPP products across multiple biomes. Remote Sensing of Environment 102(3-4): 282-292. DOI: 10.1016/j.rse.2006.02.017

Douglas EA, Stith TG, Mackay DS (2004) Heterogeneity of light use efficiency in a northern Wisconsin forest: implications for modeling net primary production with remote sensing. Remote Sensing of Environment 93(1-2): 168-178. DOI: 10.1016/j.rse.2004.07.003

Guo Z, Wang Z, Liu D (2009) Analysis of temporal and spatial features of farmland productivity in the Sanjiang plain. Transactions of the Chinese Society of Agricultural Engineering 25(1): 248-254. (In Chinese)

Gehrung J, Scholz Y (2009) The application of simulated NPP data in improving the assessment of the spatial distribution of biomass in Europe. Biomass and Bioenergy 33(4): 712-720. DOI: 10.1016/j.biombioe.2008.11.005

Xiao J, Zhuang Q, Beverly EL (2010) A continuous measure of gross primary production for the conterminous United States derived from MODIS and AmeriFlux data. Remote Sensing of Environment 114(3): 576-591. DOI: 10.1016/j.rse.2009.10.013

Huemmrich KF, Gamon JA, Tweedie CE (2010) Remote sensing of tundra gross ecosystem productivity and light use efficiency under varying temperature and moisture conditions. Remote Sensing of Environment 114(3): 481-489. DOI: 10.1016/j.rse.2009.10.003

Li G, Xin X, Wang D (2008) Estimation of grassland photosynthesis parameters based on MODIS-BASED—taking inner Mongolia as an example. Chinese Journal of Grassland 30(3): 1-7. (In Chinese)

Li Y, Zhao X, Cao G (2004) Analyses on climates and vegetation productivity background at Haibei Alpine Meadow ecosystem research station. Plateau Meteorology 23(4): 558-567. (In Chinese)

Lin X (2008) A simple introduction to LIBSVM. Available online: http://www.csie.ntu.edu.tw/~cjlin/libsvm (Accessed on 18 November, 2008)

Michael Z, Karl-Heinz E (2009) The global loss of net primary production resulting from human-induced soil degradation in drylands. Ecological Economics 69(2): 310-318. DOI: 10.1016/j.ecolecon.2009.06.014

Pontus O, Lars E (2007) Estimation of absorbed PAR across Scandinavia from satellite measurements. Part II: Modeling and evaluating the fractional absorption. Remote Sensing of Environment 110(2):240-251.DOI: 10.1016/j.rse.2007.02.020

Pu J, Li Y, Zhao L (2005) Seasonal changes of Kobresia Humilis Meadow biomass with climate factor. Acta Agrestia Sinica 13(3): 238-241. (In Chinese)

Shen Y, Xiang L (1991) The Physical Geography of Qianghai Province: 14-71, Ocean Press, Beijing. (In Chinese)

Tucker CJ, Townshend JRG, Goff TE (1985) African land-cover classification using satellite data, Science 227: 369-375. DOI: 10.1126/science.227.4685.369

Venturini V, Bisht G, Islam S (2004) Comparison of evaporative fractions estimated from AVHRR and MODIS sensors over South Florida. Remote Sensing of Environment 93(1-2): 77-86. DOI: 10.1016/j.rse.2004.06.020

Wang L, Wei Y, Niu Z (2008) Spatial and temporal variations of vegetation in Qinghai Province based on satellite data. Journal of Geographical Sciences 18(1): 73-84. DOI: 10.1007/s11442-008-0073-x

Yuan W, Liu S, Zhou G (2007) Deriving a light use efficiency model from eddy covariance flux data for predicting daily gross primary production across biomes. Agricultural and Forest Meteorology 143(3-4): 189-207. DOI: 10.1016/j.agrformet.2006.12.001

Yan H, Wang S, Wang C (2004) Impact of wind erosion on carbon cycle of fragile ecosystem in northern china. Quaternary Sciences 24(6): 672-677. (In Chinese)

Yu G, Sun X (2008) Flux measurement and research of terrestrial ecosystem in China. Science Press, Beijing. pp 597-632. (In Chinese)

Zhu W, Pan Y, He H (2006) Simulation of maximum light use efficiency for main vegetation in China. Chinese Science Bulletin 51(6): 700-706. (In Chinese)